Local structure of nitrogen-hydrogen complexes in dilute nitrides

G. Ciatto,[1,*] F. Boscherini,[2] A. Amore Bonapasta,[3] F. Filippone,[3] A. Polimeni,[4] M. Capizzi,[4] M. Berti,[5] G. Bisognin,[5,6] D. De Salvador,[5] L. Floreano,[7] F. Martelli,[7] S. Rubini,[7] and L. Grenouillet[8]

[1]*Synchrotron SOLEIL, L'Orme des Merisiers, Saint-Aubin, BP 48, 91192 Gif sur Yvette Cedex, France*

[2]*Department of Physics and CNISM, University of Bologna, V. le C. Berti Pichat 6/2, 40127 Bologna, Italy*

[3]*CNR-Istituto di Struttura della Materia (ISM), Via Salaria Km 29.5, CP 10, I-00016 Monterotondo Stazione, Italy*

[4]*CNISM-Dipartimento di Fisica, Sapienza Università di Roma, Piazzale A. Moro 2, 00185 Roma, Italy*

[5]*MATIS CNR-INFM e Dipartimento di Fisica, Università di Padova, Via Marzolo 8, 35131 Padova, Italy*

[6]*CNISM, Unità di Padova, Via Marzolo 8, 35131 Padova, Italy*

[7]*TASC-INFM-CNR, Area Science Park, S.S. 14, Km. 163.5, 34012 Trieste, Italy*

[8]*CEA-LETI, MINATEC, 17 rue des Martyrs, 38054 Grenoble Cedex 9, France*

(Received 5 December 2008; revised manuscript received 3 February 2009; published 20 April 2009)

We have investigated the structure of nitrogen-hydrogen complexes in $GaAs_{1-y}N_y$ and $In_xGa_{1-x}As_{1-y}N_y$ dilute nitride alloys by performing x-ray absorption near-edge structure spectroscopy (XANES). We simulated the spectra based on first-principles calculations of the most recent defective structures proposed in the literature for hydrogenated materials. The comparison between the experimental data and simulations allows us to clarify that the core of the defect is a complex with C_{2v} structure in the *neutral* charge state, in agreement with the expansion of the lattice parameter measured by x-ray diffraction. Our results are compatible with the presence of H satellites bound to neighboring Ga atoms but not with complexes involving more than two H atoms bound to the same N. Nevertheless, we were not able to determine uniquely the number of H satellites, which may depend on growth conditions. Strain related to the epitaxial growth has a very little effect on the XANES spectra.

DOI: 10.1103/PhysRevB.79.165205 PACS number(s): 61.05.cj, 61.66.Dk, 81.05.Ea

I. INTRODUCTION

Hydrogen (deuterium) incorporation in $GaAs_{1-y}N_y$ and $In_xGa_{1-x}As_{1-y}N_y$ provides a way to tailor the emission properties of these materials and discloses potential opportunities in defects and band-gap engineering. As a matter of fact, hydrogenation of such alloys reverses[1,2] the counterintuitive band-gap redshift caused by N incorporation,[3,4] expands dramatically the lattice parameter,[5] and restores the values of the effective mass[6] and gyromagnetic factor.[7] Moreover, all these effects are fully reversible by simple thermal annealing, which permits tuning of the emission wavelength after the growth within a range of great interest in telecommunication and photovoltaic technologies.[8] The possibility of obtaining structures with lateral band-gap variation on the micrometer scale by hydrogenating dilute nitrides using patterned masks has been recently demonstrated[9,10] and, with an improvement of miniaturization, hydrogenation will have the possibility to produce nanostructures with in-plane confinement, with potential impact in the engineering of optical circuits.[11]

The effects of hydrogenation have been accounted for by the hypothesis of formation of specific N-H complexes, and the number and location of H atoms around N has been debated in the literature for the last six years. The initial prediction of complexes involving two H atoms, one linked to N and the other to a neighboring Ga in an in-line configuration (called H_2^*) (Refs. 12–14) has been excluded by infrared-absorption (IR) measurements[15] which have never provided evidence of a Ga-H bond-stretching mode in $GaAs_{1-y}N_y$. At the same time, the presence of a different complex involving two H atoms linked to the same N in a C_{2v} geometry was proposed:[16,17] such complex accounted for the presence of two N-H stretching modes[15] in the absorption spectrum. Recently, by using N *K*-edge x-ray absorption near-edge structure spectroscopy (XANES) and full multiple-scattering (FMS) simulations based on density-functional theory (DFT) calculations, we were able to provide firm evidence that the basic structure of most complexes is the C_{2v} one either in a symmetric or asymmetric configuration.[18] Straight after, two different groups published calculations[19,20] showing that a canted or asymmetric C_{2v} complex [see Fig. 1(a)], described by the C_{1h} symmetry, has vibrational properties consistent with the IR experiment.

Nowadays, it is common opinion that C_{2v} complexes should be in the neutral charge state [C_{2v}^0, Fig. 1(a)] since this is the only one which yields recovery of the lattice con-

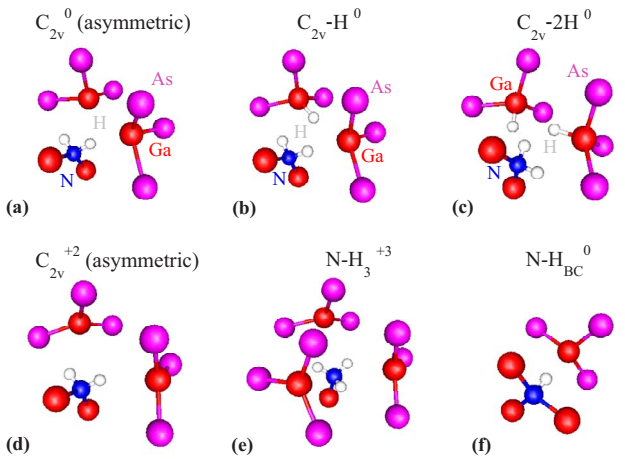

FIG. 1. (Color online) Sketch of the different N-H complexes under investigation.

TABLE I. Sample characteristics and measured $\Delta a_\perp / a_0$ parameter (see text) along with predictions based on selected N-H complexes models; for samples A and B, a_0 is defined as the GaAs lattice parameter while for sample C it is defined as the lattice parameter of a $In_{0.037}Ga_{0.963}As$ alloy. The last column contains the values of $\Delta a_\perp / a_0$ normalized to the N concentration.

Sample (or model)	N %	In %	Thickness (nm)	Treatment	$\Delta a_\perp / a_0$ (%)	$(\Delta a_\perp / a_0)/(\%N)$
A	1.22 ± 0.02	0	223 ± 10	Deuterated	0.17 ± 0.01	0.14 ± 0.01
B	1.22 ± 0.02	0	223 ± 10	Deut+anneal	0.0 ± 0.1	0.00 ± 0.08
C	3.43 ± 0.06	3.70 ± 0.15	149 ± 3	Hydrogenated	0.35 ± 0.04	0.10 ± 0.01
C_{2v}^0	3.12	0	66 atoms	DFT	0.00 ± 0.01	0.000 ± 0.003
C_{2v}-H^0	3.12	0	67 atoms	DFT	0.42 ± 0.01	0.135 ± 0.003
C_{2v}-$2H^0$	3.12	0	68 atoms	DFT	0.39 ± 0.01	0.125 ± 0.003

stant comparable with that measured via x-ray diffraction.[5,21] It is worth remarking here that, despite this assumption, our previous XANES simulations were done for doubly charged complexes [C_{2v}^{+2}, Fig. 1(d)] and no analysis of neutral complexes has been done up to now. Due to the rather different distances between Ga atoms surrounding the N one predicted for charged and neutral C_{2v} complexes,[22] the XANES spectrum of neutral C_{2v} could be *a priori* different from that of charged C_{2v} and incompatible with the experimental data: this point urges to be clarified.

Moreover, recent high-resolution x-ray diffraction (HRXRD) experiments performed by some of us[21] have provided evidence of compressive strain in as-deuterated samples which cannot be accounted for by the formation of bare C_{2v} complexes, and a nuclear reaction analysis/channeling investigation[23] showed that the ratio between H and N atoms concentrations is close to three (instead of two). DFT calculations[22] demonstrated the stability of structures involving additional H "satellite" atoms (one or two) in the proximity of the C_{2v} defect [Figs. 1(b) and 1(c)], such structures are predicted to produce compressive strain in good agreement with that measured by HRXRD.[21] Even if these last results speak for the presence of H satellites around the core complex, several issues still remain controversial; as a matter of fact, theoretical calculations predict that the final step of the hydrogenation process should involve two H satellites (i.e., four H atoms in total),[22] with an expected H/N ratio of four, which is different from the one experimentally determined.[23] Even for the case of C_{2v} complexes with additional H satellites, no XANES simulation is available in the literature at the present. Furthermore, in a very recent and detailed study, Kleekajai *et al.*[24] were able to account for all the features observed in the IR spectrum (including wagging modes) based on the only asymmetric C_{2v} core, at least for samples hydrogenated at 300 °C. Finally, based on secondary-ion-mass spectroscopy and photoluminescence (PL) data, Buyanova *et al.*[25] suggested that the H/N ratio in $GaAs_{1-y}N_y$ and $GaP_{1-y}N_y$ should be larger (from three to five), and the formation of complexes involving the presence of up to five H atoms correlated with a single nitrogen.

In the present paper we performed detailed FMS simulations of the N *K*-edge XANES for different nitrogen local configurations, exploring the most recent complex structures proposed in the literature. In particular, considering C_{2v} complexes, we studied the effect of different charge states and the tetragonal distortion of the unit cell due to the epitaxial growth on GaAs. Also, we investigated the presence of additional H atoms yielding H/N ratio ≥ 3, both directly linked to N atoms and in satellite position close to the core of the defect. We compared the simulations to experimental spectra of deuterated/hydrogenated $GaAs_{1-y}N_y$ and $In_xGa_{1-x}As_{1-y}N_y$ samples. Our method is based on calculation of atomic supercells around a central N atom performed by using DFT. Such method is becoming a powerful tool in the study of the local structure of defects in semiconductors[26] and, after publication of our first results on N-H complexes in dilute nitrides,[18] similar approaches have been successfully used, for example, in the study of N-doped oxides[27] and indium oxynitrides.[28]

II. EXPERIMENTAL AND THEORETICAL METHODS

We measured two $GaAs_{1-y}N_y$ samples (A and B) and one $In_xGa_{1-x}As_{1-y}N_y$ sample (C), their characteristics are shown in Table I.

A $GaAs_{1-y}N_y$ epilayer was grown by solid source molecular-beam epitaxy on (001) GaAs substrates with an rf plasma source for N. Sample growth was performed at 500 °C after having grown a 500-nm-thick GaAs buffer layer at 600 °C. Nitrogen was mixed in the plasma with argon and the rf source power used was in the 60–70 W range. Postgrowth thermal annealing at 660 °C for 60 min was used in order to improve the optical properties of the samples. The thickness of the samples and the nitrogen concentration were determined by HRXRD, based on a previous verification of the validity of the Vegard's law by means of nuclear reaction analysis (NRA) measurements.[29] After the growth, the epilayer was deuterated. Deuteration was performed with a Kaufman source at 300 °C and D fluences $d_D = 5 \times 10^{18}$ ions/cm^2 was employed in order to obtain full N passivation. The samples were irradiated with an ion-beam current density of 38 μA/cm^2. Then, while one piece of the epilayer (sample A) was not treated anymore, a second peace (sample B) was softly annealed at 250 °C for ≈ 13 h.

Sample C was grown on (001) GaAs substrate by gas-source molecular-beam epitaxy using a radio-frequency plasma source, growth temperature was 430 °C (Ref. 30); thermal annealing was performed in a rapid thermal anneal-

ing (RTA) furnace under N_2 flow at 700 °C for 300 s. Annealing strongly enhances the photoluminescence signal. Indium concentration was determined by Rutherford backscattering spectrometry (RBS), nitrogen concentration, and sample thickness by HRXRD (as for the ternary samples). After growth, hydrogenation was performed with a Kaufman source at 300 °C and H fluences $d_H = 5.8 \times 10^{18}$ ions/cm^2, with beam current density of 32 μA/cm^2.

All epilayers were found by HRXRD reciprocal space mapping to be pseudomorphic to the GaAs substrate. Measurements of the lattice parameter were carried out using a Philips X'Pert PRO MRD diffractometer. The x-ray wavelength was $\lambda_{Cu\,K\alpha 1} = 1.540\,56$ Å and the angular acceptance was 12 arc s (triple axis configuration). PL was excited with a neodymium-vanadate laser ($\lambda = 532$ nm) and spectrally analyzed by a single grating 0.75-m-long monochromator coupled to a cooled InGaAs linear array detector. PL spectra were taken at a temperature of 10 K or at room temperature. NRA-channeling measurements,[29] together with polarization dependent N *K*-edge XANES,[31] guarantee that N is totally substitutional to As in the zinc-blende lattice. The fact that samples A and B have been deuterated instead of hydrogenated is related to the needs of stoichiometric characterization previously performed on the same samples;[23] however deuterium modifies electronic and structural properties of dilute nitrides as hydrogen does so that the different postgrowth treatment does not affect the results presented in this work.[32] In the following, we will always use "H" in the complex labels.

N *K*-edge XANES measurements were performed at the ELETTRA synchrotron-radiation facility in Trieste at the ALOISA beamline.[33] The photon flux on the sample was of the order of 5×10^{11} photons/s on a focal spot of 0.2×0.5 mm^2. The value of the undulator gap was synchronized with the photon energy selected by the monochromator. Fluorescence detection was used in order to guarantee bulk sensitivity. The setup is based on the use of a windowless hyperpure Ge detector with a detection area of ≈ 100 mm^2 placed in the horizontal plane at 90° to the impinging photon beam at a distance of ≈ 5 mm from the sample. The high brilliance photon beam coupled to the highly efficient detection scheme is mandatory in order to record good signal-to-noise ratio spectra from dilute elements in the soft x-ray range. A test measurement performed on a N-free sample (not shown) demonstrated that the N contamination on the surface is definitely negligible with respect to the signal originating from the bulk. The energy position of the absorption edge in all experimental spectra reported in the present paper has been calibrated by collecting the XANES in real time with gas absorption spectroscopy on the N_2 *K* edge using specific instrumentation available at the ALOISA beamline.[33] As explained in detail in a previous paper,[34] such procedure guarantees energy calibration of the XANES spectra with a precision of ± 15 meV.

XANES spectra were simulated in a real-space FMS approach based on the Green's function calculations in the complex plane using the FEFF8 code.[35] Such code employs a Barth-Hedin formulation for the exchange-correlation part of the potential and the Hedin-Lundqvist self-energy correction. Calculation of the potential was performed by using a self-consistent field within a 5.2 Å radius, a distance which includes the second coordination shell of a central nitrogen in hydrogenated GaAsN for any N-H complex analyzed in this work (such radius is bigger than the one previously employed[18]). Atomic coordinates for each N-H complex were taken from DFT calculations,[22] repeating eight times a 64-atoms supercell and translating the positions in order to drive a N atom to the center of the cell. Clusters exploited in the FMS calculations consisted, indeed, of 512 atoms for GaAsN, 520 for monohydrogen complexes, 528 for dihydrogen complexes, and 536 and 544 atoms for complexes involving three and four H atoms correlated with N, respectively. The full multiple-scattering radius was fixed to 20 Å in order to enclose all input atoms without using any extra scattering paths. The use of such large clusters is mandatory to reproduce the region of the absorption spectrum close to the edge, where the photoelectron mean-free path can reach a few tens of angstroms. In the modeling of epilayers pseudomorphically strained on the substrate, we considered all possible orientations of the complexes and averaged them according to their statistical abundance. DFT calculations were performed in a supercell approach by using separable *ab initio* pseudopotentials.[36,37] Geometry optimization has been performed by fully relaxing the atomic positions in 64-atom supercells with the PWSCF code.[38] Further details on the theoretical methods have been reported elsewhere.[16,17]

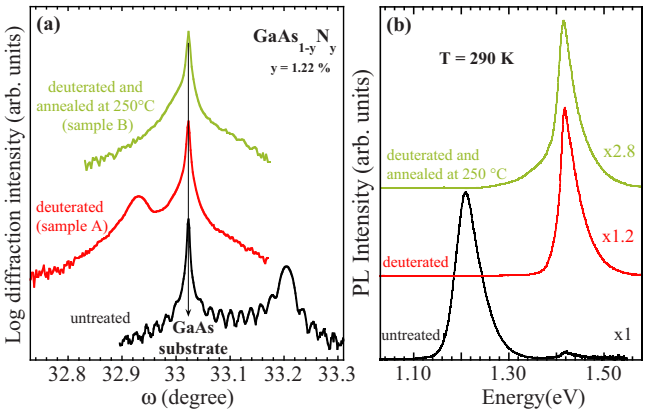

FIG. 2. (Color online) (a) HRXRD (004) rocking curves for the $GaAs_{0.9878}N_{0.0122}$ epilayer before deuteration (bottommost line), after deuteration (middle line, sample A), and after deuteration followed by a mild thermal annealing at 250 °C (topmost line, sample B); (b) corresponding PL spectra.

III. RESULTS AND DISCUSSION

A. X-ray diffraction and optical spectroscopy

For clearness of exposition, we show in Fig. 2 HRXRD and PL data for samples A and B already discussed in a previous work[21] while Fig. 3 shows the same data for sample C.

In Fig. 2(a), the (004) rocking curves (RCs) of the as-grown $GaAs_{0.9878}N_{0.0122}$ epilayer (bottommost curve), and of the same sample both after deuteration (middle curve, sample A) and subsequent moderate annealing (250 °C, 13 h) (topmost curve, sample B) are shown. By comparing the

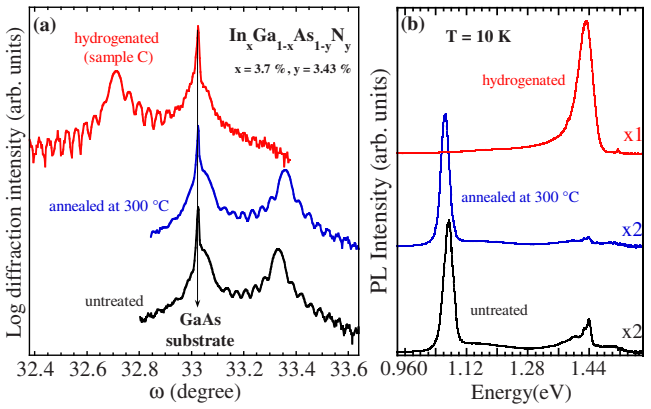

FIG. 3. (Color online) (a) HRXRD (004) rocking curves for a $In_{0.037}Ga_{0.963}As_{0.9657}N_{0.0343}$ epilayer with $x=3.70\%$ and $y=3.43\%$ before hydrogenation (bottommost curve), after hydrogenation (topmost curve, sample C), and for a piece of epilayer undertaking the same annealing procedure as during hydrogenation but with the H source switched off (middle curve); (b) corresponding PL spectra.

RCs of the as-grown and of the deuterated samples, it is clear that the deuteration process is the origin of the $GaAs_{1-y}N_y$ epilayer (004) Bragg-peak shift from larger to smaller angles with respect to the substrate peak. This means that, after the formation of N-H complexes, the original epilayer tensile strain, due to the insertion of substitutional N in GaAs, is reversed into a compressive one. Moreover, previous HRXRD measurements on several other fully hydrogenated or deuterated $GaAs_{1-y}N_y$ films, including sample A, have shown that the compressive strain induced by hydrogenation only depends on the initial N concentration (i.e., on the tensile strain) in the nonhydrogenated as-grown material.[21] In particular, it was deduced that

$$\frac{a_{D\perp}-a_0}{a_0}=\frac{(5.24\pm 0.27)\ \text{Å}}{a_0}y, \tag{1}$$

where $a_{D\perp}$ is the lattice parameter (in angstroms) along the growth direction of the $GaAs_{1-y}N_y$ epilayers after the hydrogenation, a_0 is the lattice parameter of bare GaAs, and y is the N concentration. In addition, (004) HRXRD spectra collected *in situ* during annealing of the deuterated epilayer have shown that, after moderate annealing (250 °C, 13 h), the $GaAs_{1-y}N_y$ Bragg peak almost completely disappears [Fig. 2(a), topmost curve], i.e., its strain is zero.[21]

In Fig. 2(b) we show the corresponding PL spectra for the sample exposed to these different postgrowth treatments. The intense band that peaked at 1.21 eV in the bottommost spectrum, recorded on the untreated sample, is due to carriers recombining in the $GaAs_{1-y}N_y$ layer. The much less intense band at 1.42 eV is caused by carrier recombination in the GaAs buffer layer. Irradiation with deuterium changes dramatically the PL spectrum (middle line). No carrier recombination can be observed from the $GaAs_{1-y}N_y$ band-gap energy and the wavelength of all emitted photons is blueshifted at the band-gap energy of GaAs. This phenomenon has been reported in previous works and it is ascribed to the electronic passivation of nitrogen determined by the formation of the N-H complexes discussed in Sec. I. The topmost spectrum refers to the same deuterated sample described above after a mild thermal annealing at 250 °C. Apart from a modest broadening of the PL linewidth and a decrease in the PL signal, no change in the PL peak energy can be detected thus indicating that nitrogen atoms are still passivated despite of the major changes observed in the x-ray diffraction pattern. On the basis of these results it was established that both the optical passivation of N and its tensile strain neutralization are consequence of the formation of the same N-H complex, characterized by the C_{2v} structure suggested by XANES,[18,23] while the strain overshooting is possibly due to the presence of a more weakly bound satellite H atom.[21,23]

With the help of RC simulations, we can measure the strain status of samples A and B through their perpendicular mismatch, i.e., the quantity:

$$\left(\frac{\Delta a_\perp}{a_0}\right)_{(A,B)}=\frac{a_\perp-a_0}{a_0}, \tag{2}$$

where $a_\perp$ is the lattice parameter along the growth direction of the $GaAs_{1-y}N_y$ epilayer while a_0 is the lattice parameter of GaAs. Moreover, based on the linear dependence of $\frac{\Delta a_\perp}{a_0}$ on N concentration, we can consider also the perpendicular mismatch normalized to N concentration y:

$$\left(\frac{\Delta a_\perp}{a_0}\right)_{(A,B)(\%N)}=\left(\frac{\Delta a_\perp}{a_0}\right)/(\%N). \tag{3}$$

This last quantity, which has been reported in the last column of Table I, permits an easy comparison between experimental and theoretically calculated perpendicular mismatches. As for sample A, $(\Delta a_\perp/a_0)/(\%N)$ is $=-0.39$ before deuteration and $=0.14$ after deuteration while in sample B (deuterated and annealed) $(\Delta a_\perp/a_0)/(\%N)$ is ≈ 0.00. DFT calculations, performed on supercells with 3.12% N concentration, predict $(\Delta a_\perp/a_0)/(\%N)=-0.346$ for untreated $GaAs_{1-y}N_y$, and $(\Delta a_\perp/a_0)/(\%N)=0.000$, 0.135, and 0.125 for C_{2v}^0, C_{2v}-H^0, and C_{2v}-$2H^0$ complexes, respectively,[22] so that the C_{2v}-H^0 and C_{2v}^0 models give the best agreement with HRXRD results for samples A and B, respectively. Such association would be compatible with the removal via annealing of the less tightly bound D atom from a primitive C_{2v}-H defective structure, which leaves a C_{2v} core, and would account for NRA measurements[23] which give a D/N ratio ≈ 3 for sample A and ≈ 2 for sample B.

In Fig. 3(a) the (004) RCs of a quaternary alloy of $In_xGa_{1-x}As_{1-y}N_y$ with $x=3.70\%$ and $y=3.43\%$ are shown for (i) the as-grown epilayer (bottommost curve), (ii) the same sample after hydrogenation (topmost curve, sample C), or (iii) thermal annealing in the same conditions as during hydrogenation (middle curve). First of all we can note that the strain status of the as-grown sample is tensile, despite the non-null In content ($x=3.70\%$). This is due to the fact that the compensation ratio between In and N is ≈ 2.8 (Ref. 29) (i.e., the tensile strain induced by 1% N is compensated by the compressive strain induced by 2.8% In) while, for sample C, $x/y=1.08$. Also in this case hydrogenation switches the strain from tensile (bottommost curve) to compressive (topmost curve) while the annealing performed on an as-grown piece of epilayer in the same conditions as during hydroge-

nation but with the H source switched off (middle curve) does not bring about an increase in the lattice parameter. If we calculate the perpendicular mismatch $\frac{\Delta a_\perp}{a_0}$ for the quaternary epilayer considering as a_0 the lattice parameter of the GaAs substrate, almost specular values for the as-grown and hydrogenated states are obtained (−0.84% for the former and 0.83% for the latter, −0.91% for the annealed sample). Nevertheless, if we want to highlight the neat effect of N and H on the lattice parameter, we have to take into account the presence of In. To this purpose, we redefine the perpendicular mismatch for sample C in the following way:

$$\left(\frac{\Delta a_\perp}{a_0}\right)_{(C)} = \frac{a_\perp - a_{\perp \mathrm{InGaAs}}}{a_{\perp \mathrm{InGaAs}}}, \tag{4}$$

where $a_\perp$ and $a_{\perp \mathrm{InGaAs}}$ are the out-of-plane lattice parameter of the quaternary epilayer and the out-of-plane lattice parameter of an $In_xGa_{1-x}As$ layer with the same In content as sample C, respectively. For relatively small x concentrations, Eq. (3) can be rewritten as

$$\frac{a_\perp - a_{\perp \mathrm{InGaAs}}}{a_{\perp \mathrm{InGaAs}}} \approx \frac{a_\perp - a_{\perp \mathrm{InGaAs}}}{a_0} = \frac{a_\perp - a_0}{a_0} - \frac{a_{\perp \mathrm{InGaAs}} - a_0}{a_0}, \tag{5}$$

where the first term of the last member is the measured mismatch with respect to the GaAs substrate while the second term can be calculated knowing the x concentration of sample C (x=3.70%, determined by RBS), and exploiting the Vegard law and elasticity theory.[39] The N normalized perpendicular mismatch, for sample C, is defined in the same way used for samples A and B:

$$\left(\frac{\Delta a_\perp}{a_0}\right)_{(C)(\%N)} = \left(\frac{\Delta a_\perp}{a_0}\right)/(\%N). \tag{6}$$

For sample C, the last two columns of Table I report the values determined using Eqs. (3) and (6), respectively. The resulting value of $(\Delta a_\perp/a_0)/(\%N)$ for the quaternary epilayer is =−0.39 in the as-grown state and 0.10 after hydrogenation. The $(\Delta a_\perp/a_0)/(\%N)$ value for sample C is smaller than for sample A (0.14), and closer to the value predicted in case of formation of C_{2v}-$2H^0$ complexes (0.125): this finding supports the formation of complexes giving less compressive strain than the C_{2v}-H^0 one in sample C.

Inspecting PL data for sample C [Fig. 3(b)], it is straightforward that hydrogenation brings about a dramatic opening of the band gap as already observed for other samples. The PL peak corresponding to the hydrogenated epilayer (at energy =1.431 eV) is not far from the value expected for the band gap of a $In_{0.037}Ga_{0.963}As$ alloy at 10 K (1.484 eV).[40] The PL intensity of the hydrogenated sample is roughly twice as the one of the untreated sample. The higher PL intensity observed in the hydrogenated sample is attributed to H passivation of nonradiative recombination centers, which spoil optical efficiency in the untreated material. PL recorded on a piece of sample C exposed to the same thermal treatment as during hydrogenation but with the H source switched off (referred to as "annealed at 300 °C" in Fig. 3) shows no intensity decrease in the main peak with respect to the spectrum of the untreated sample and only a minor redshift of the corresponding energy (smaller than 0.01 eV). This last observation confirms that the main changes in the material properties observed upon the hydrogenation procedure (both optical and structural, reported in Figs. 3(b) and 3(a), respectively) are a neat effect of the interaction of hydrogen atoms with the crystal lattice. The 0.01 eV redshift likely origins from a slightly higher N concentration in the piece of sample exposed to annealing; this is also confirmed by the higher tensile strain measured by HRXRD on the same annealed piece [Fig. 3(a)]. The PL bands in the 1.35–1.5 eV energy range observed for the untreated sample are due to a fraction of N (about 0.15%) incorporated and/or diffused in the GaAs buffer layer. The low-energy tail in the PL spectrum of the hydrogenated sample and the 1.1–1.35 eV background region of the nonhydrogenated ones origin from defect states related to several causes: the increased degree of structural disorder induced by the higher N concentration with respect to samples A and B, and the incorporation of In, and the higher concentration of point defects expected because of the lower growth temperature.[41–43]

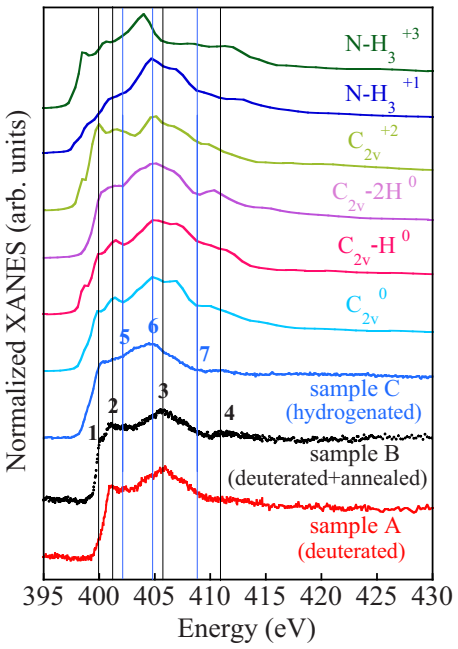

FIG. 4. (Color online) N K-edge XANES simulations for selected N-H complexes having an asymmetric C_{2v} core and for $N\text{-}H_3$ complexes (continuous line) compared to three experimental spectra (dots, at the bottom); a very small energy shift of −0.25 eV is applied to all simulations for a better matching with the experimental data.

B. XANES

In Fig. 4 we show FMS simulations of the N K-edge XANES performed in presence of neutral asymmetric C_{2v} complexes (C^0_{2v}), neutral asymmetric C_{2v} complexes decorated with one (C_{2v}-H^0), and two (C_{2v}-$2H^0$) H satellites, along with the previously published simulation[18] for the doubly charged complex (C^{+2}_{2v}) and simulations for complexes with three H atoms bound to the same N one in the +1 and

+3 charge states [N-H_3^{+1} and N-H_3^{+3}, see Fig. 1(e)]. In order to mimic as close as possible the experimental situation, we took into account the effect of the tetragonal distortion of the unit cell due to the pseudomorphic growth on the substrate. Several charge states were explored for all the complexes under study but only the most stable ones for each configuration are reported here. Simulations are compared to the experimental spectra for the ternary samples A and B, already reported previously,[23] and for sample C, which contains a small percent of In.

If we compare the spectrum of sample B with the simulations, we note that the line shape and energy position of the main spectral features (evidenced by vertical lines and by the numbers 1–4) are very well reproduced by the simulation based on the C_{2v}^0 model, the only mismatch coming from the fact that the experimental main peak 3 is less structured than in the simulation. The simulation for such neutral complex mimics the experimental data even better than the one based on the C_{2v}^{+2} complex presented in our previous work,[18] in particular for what concerns features 1 and 2, the relative amplitude of which is inverted in case of the doubly charged complex. The difference between the XANES line shape of the simulations for C_{2v}^0 and C_{2v}^{+2} complexes can be attributed to the fact that in the former case two dangling bonds are induced on the Ga atoms involved in the broken Ga-N bond so that these Ga atoms interact forming a weak Ga-Ga bond, and their interatomic distance (≈3.24 Å) is sensibly shorter than the distances between the other Ga atoms. On the contrary, in the case of the C_{2v}^{+2} complex the same Ga-Ga distance is much longer (≈5.02 Å) since the Ga atoms which carried the dangling bond have lost their unpaired electron and cannot form any Ga-Ga bond.[20,22] Moreover, the angle formed by the same two Ga atoms and centered on N is very different for the two charge states, being ≈61° for C_{2v}^0 and ≈89° for C_{2v}^{+2}: this difference in interatomic distances and angles between atoms which are located very close to N is directly reflected in a XANES change due to its strong local sensitivity. The association of sample B with the C_{2v}^0 model accounts for the null strain measured by HRXRD (Ref. 21) (Sec. III A), and the D/N ratio ≈2 measured by NRA (Ref. 23) on this sample.

The simulation for the C_{2v}-H^0 complex, instead, is very similar to the one for the bare C_{2v}^0 in the same charge state apart for a little shoulder positioned at lower energy than feature 1. In this case, in fact, the distance between the two Ga atoms involved in the breaking of Ga-N bonds is ≈3.92 Å, i.e., closer to the value for C_{2v}^0 than for C_{2v}^{+2}; this is also true for the distances between N and the same two Ga atoms, and for the angle formed by these two Ga atoms and N, centered on N (≈72°): briefly, apart from the absence of a third H atom, the local structure of N in a C_{2v}^0 complexes is closer to C_{2v}-H^0 than to C_{2v}^{+2}. The experimental spectrum of sample A, which is in a configuration with D/N ratio ≈3 according to NRA investigation, is very similar to the one of sample B, the only essential difference being the absence of feature 1. The hypothesis of formation of C_{2v}-H^0 complexes in the as-deuterated $GaAs_{1-y}N_y$ sample, which accounts for HRXRD and NRA data, is also compatible with XANES results for the following reasons: the match of the simulations for C_{2v}^0 and C_{2v}-H^0 complexes, the resemblance of the experimental spectra for samples A and B, and, finally, the intrinsic difficulty in reproducing the energy range around and below feature 1 where the relatively large mean-free path of the photoelectron makes us sensible to medium-range order correlations larger than the maximum reasonable cluster dimension that we can employ in the analysis. Nevertheless, some doubt related to the absence of feature 1 in the experimental spectrum of sample A still remains. If we consider other configurations yielding D/N ratio ≈3, in particular N-H complexes with three H atoms bound to the same N (N-H_3), the corresponding FMS simulations (the two topmost curves in Fig. 4) are rather at variance with the experimental spectra. This allows us to discard such configurations, in agreement with theoretical results which predict that complexes with three N-H bonds are metastable or unstable.[22] We show here only the simulations for the +1 and +3 charge states (N-H_3^{+1} and N-H_3^{+3}), with the simulation for the +2 state being very similar to that for the +3 one.

The experimental spectrum of sample C, grown at lower temperature than A and B, presents some differences compared to the others. First, there is a remarkable redshift (of almost 1 eV) of the main peak at ≈404.8 eV (referred to as feature 6) with respect to the one of sample B. The energy calibration procedure described in Sec. II assures that differences in the energy position of the features reported in Fig. 4 do not come from an artifact but originate from the physics of the samples. A more detailed inspection of sample C spectrum reveals that the position of the first change in slope (feature 1) corresponds to the one of sample B, with which the peak referred to as feature 2 is absent, and the presence of a second slope change at 402.1 eV (indexed as feature 5). Shifts of the absorption edge in $In_xGa_{1-x}As_{1-y}N_y$ samples could *a priori* originate as a consequence of preferential binding of In atoms to N driven by minimization of the strain energy related to this short-range ordering (SRO) configuration.[44,45] However, these shifts are usually tiny and, according to Lordi *et al.*,[45] in a $GaAs_{1-y}N_y$ sample with $y=3\%$ the N *K* edge should shift by 0.1–0.2 eV upon incorporation of 30% In atoms and by further 0.1 eV upon annealing when the average number of In atoms nearest neighbors (NN) to N varies from one to three. In the case of our sample C, which was already measured by In *K*-edge extended x-ray-absorption fine structure before hydrogenation,[46] In concentration is only 3.7% and SRO brings only a 10% of In atoms in NN position with respect to N; this is confirmed by the fact that the N *K*-edge XANES spectrum of sample C before hydrogenation (not shown here) presents virtually no difference compared to that of a pure $GaAs_{1-y}N_y$.[46] This means that, in the case of our sample, In incorporation and ordering should bring about a shift of the N edge of the order 0.05 eV and cannot account for a shift of 1 eV. All these considerations suggest that the differences between the XANES of samples B and C reported in Fig. 4 come from different structural changes induced by hydrogenation.

If we compare the experimental XANES of sample C to the FMS simulation for the C_{2v}-$2H^0$ complex, it is evident that the simulation is able to reproduce the energy position of feature 1, the absence of feature 2, and the change in slope referred to as feature 5. Moreover, it well reproduces the position of the main peak (feature 6) and the subsequent

valley at 408.8 eV (feature 7), giving an overall line shape in better agreement with the experimental spectrum than the simulations for the C^0_{2v} and C_{2v}-H^0 configurations. The latter two simulations, in fact, show a peak in position 2 which is not present in the spectrum of sample C, and the "center of mass" of their main peak at ≈405.7 eV is not aligned with the experimental feature 6. The differences between the simulations of C_{2v}-H^0 (C^0_{2v}) and C_{2v}-$2H^0$ complexes are likely due to the longer distance between the two Ga atoms involved in the breaking of the Ga-N bond (≈4.26 Å) predicted in the latter case, and related to the H saturation of the two dangling bonds induced on Ga, and to the longer distances between such Ga atoms and the N one, even if the value of the angle centered on N (≈74°) is close to the one predicted for the case of C_{2v}-H^0. Although such differences are rather subtle, these observations suggest the formation of C_{2v}-$2H^0$ complexes in sample C. Such hypothesis is in agreement with theoretical predictions according to which the C_{2v}-$2H^0$ complex should be the final product of the hydrogenation process,[22] and with the smaller N-normalized strain mismatch measured by HRXRD on this sample (Sec. III A) with respect to previously published results.[21] Nevertheless, the slight overestimation of the $(\Delta a_\perp / a_0)/(\%\mathrm{N})$ value done even by the C_{2v}-$2H^0$ model suggests that a fraction of minority complexes yielding smaller or null compressive strain and/or a small fraction of residual N atoms which do not form complexes could be present, as well.

The formation of complexes with a different number of satellites in samples A and C can be due to different acceptors concentrations in the untreated *p*-type material caused by the different growth conditions (in particular the substrate temperature, which was kept lower during the growth of sample C). As a matter of fact, the creation and diffusion of H^+ ions in the material during the hydrogenation process is driven by the need of compensating the acceptors, and the formation of N-H complexes when N and the surrounding Ga atoms trap the diffusing H^+ ions is likely influenced by the acceptors concentration.

In Fig. 5 we show simulations done for untreated $GaAs_{1-y}N_y$, for monohydrogen N-H_{BC} complexes [Fig. 1(f)] in neutral or charged states, and a replication of the simulations for the C^0_{2v} complex (referred to as "epitaxial") and the N-H_3^{+1} complex already showed above. It is clear that local configurations with zero, one, two, and three H atoms bound to N have very different line shapes, and show progressive broadening and intensity homogenization in the near-edge region (396–415 eV). A core of two atoms bound to N in a C^0_{2v} configuration (possibly decorated by H satellites) is necessary in order to obtain a reasonable agreement with the experimental data, and the evolution of simulated spectra as a function of the number of H nearest neighbors discourages the hypothesis of formation of complexes involving more than three atoms bound to the same N. We already showed in our previous work[18] that different dihydrogen N-H complexes (not shown here) are not able to reproduce the experimental spectra, either. We also show in Fig. 5 the XANES simulation performed for the C^0_{2v} complex embedded in a bulk crystal, i.e., without taking into account the tetragonal distortion of the unit cell due to the pseudomorphic epitaxial growth: simulations for relaxed and strained epilayers are

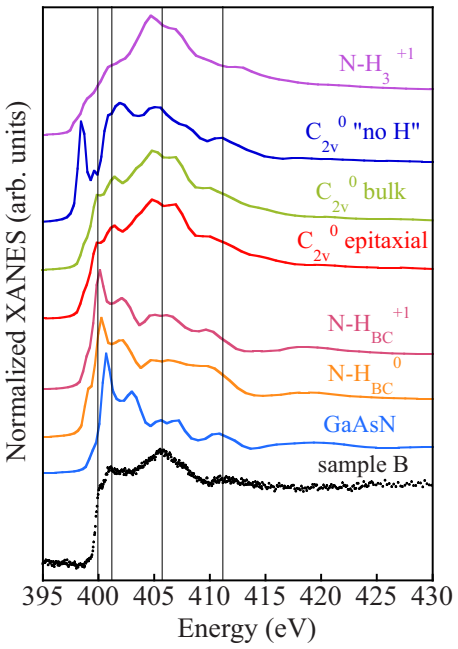

FIG. 5. (Color online) N *K*-edge XANES simulations (continuous line) for pure $GaAs_{1-y}N_y$, monohydrogen bond-centered complexes (N-H_{BC}), dihydrogen C^0_{2v} complexes in a bulk or strained crystal, N-H_3^{+1} complex, and a C^0_{2v} complex where H atoms have been artificially removed from the structure. The experimental spectrum of sample B is replicated at the bottom of the figure (dots).

virtually identical. This last point well illustrates the potentiality of XANES in the investigation of the local structure of defects in crystals and the complementarity with another important structural tool such as infrared spectroscopy. If on the one hand IR is potentially more sensitive to the presence of minority complexes since it does not limit to give average structural information, on the other hand strain leads to a broadening of the spectroscopic features and complicates the interpretation of the IR data,[47] which is not the case for XANES.

Finally, considering the influence of the interatomic distances between Ga atoms on the XANES line shape for the different N-H complexes discussed above, one may wonder whether the effects of H incorporation on the spectra limit to changes related with the redistribution of the heavier neighboring atoms. In order to clarify this point, we performed a simulation taking a C^0_{2v} cluster and arbitrarily removing all H atoms from the input list without relaxation of the other atom positions. This last simulation (referred to as C^0_{2v} "no H" in Fig. 5) gives again a rather different line shape compared to that of the C^0_{2v} complex and, in particular, a sharp pre-edge peak at 398.43 eV which is not observed experimentally. This indicates that the presence of hydrogen itself, despite its very low backscattering power, has a neat effect on the near-edge absorption cross section, which is yet another clue of the important influence of multiple scattering on the XANES signal.[26]

IV. CONCLUSIONS

We performed detailed XANES FMS simulations for different N-H complexes in hydrogenated $GaAs_{1-y}N_y$ taking

into account the effects of different charge states, presence of satellite H atoms, and epitaxial strain. We provided evidence that the actual complex which forms both in hydrogenated (deuterated) $GaAs_{1-y}N_y$ and $In_xGa_{1-x}As_{1-y}N_y$ is characterized by an asymmetric C_{2v} core structure with two H atoms bound to the same N, and that it is in the neutral charge state. A very good correspondence has been found between the XANES spectrum of a deuterated sample subsequently annealed at 250 °C for 13 h and the simulation for the bare neutral C_{2v} complex (C_{2v}^0), in agreement with the results of NRA and HRXRD experiments.

The presence of further H atoms (satellites) decorating the C_{2v} core and saturating Ga dangling bonds in as-hydrogenated (deuterated) samples recently proposed based on DFT calculations is compatible with XANES results, even if we were not able to uniquely determine the number of H satellites, which may vary upon different growth conditions. The experimental XANES spectrum of an as-deuterated $GaAs_{1-y}N_y$ sample with $y=1.22\%$ is closer to the FMS simulations performed for complexes with one (C_{2v}-H^0) or zero (C_{2v}^0) H satellites, being these two simulations very similar from each other; the first option would give a H/N ratio of three, in agreement with recent NRA results on the same sample. Instead, the XANES spectrum of an as-hydrogenated $In_xGa_{1-x}As_{1-y}N_y$ sample with $y=3.43\%$ and $x=3.7\%$ presents a significant energy shift of some spectral features, and it is better reproduced by a simulation performed in presence of two H satellites around the C_{2v} core (C_{2v}-$2H^0$). In any case, we can exclude the formation of complexes with three H atoms bound to the same N.

Finally, we have shown that the tetragonal distortion of the unit cell due to the pseudomorphic growth on the substrate has little effect on the XANES spectra simulated in presence of N-H complexes.

ACKNOWLEDGMENTS

We acknowledge support by the European Community—Research Infrastructure Action under the FP6 "Structuring the European Research Area" Programme for measurements at Elettra.

*Corresponding author; gianluca.ciatto@synchrotron-soleil.fr

[1] A. Polimeni, G. Baldassarri Höger von Högersthal, H. M. Bissiri, M. Capizzi, M. Fischer, M. Reinhardt, and A. Forchel, Phys. Rev. B **63**, 201304(R) (2001).
[2] G. Baldassarri Höger von Högersthal, H. M. Bissiri, A. Polimeni, M. Capizzi, M. Fischer, M. Reinhardt, and A. Forchel, Appl. Phys. Lett. **78**, 3472 (2001).
[3] M. Weyers, M. Sato, and H. Ando, Jpn. J. Appl. Phys. **31**, L853 (1992).
[4] T. Taliercio, R. Intartaglia, B. Gil, P. Lefebvre, T. Bretagnon, U. Tisch, E. Finkman, J. Salzman, M. A. Pinault, M. Laugt, and E. Tournié, Phys. Rev. B **69**, 073303 (2004).
[5] A. Polimeni, G. Ciatto, L. Ortega, F. Jiang, F. Boscherini, F. Filippone, A. Amore Bonapasta, M. Stavola, and M. Capizzi, Phys. Rev. B **68**, 085204 (2003).
[6] A. Polimeni, G. Baldassarri Höger von Högersthal, F. Masia, A. Frova, M. Capizzi, S. Sanna, V. Fiorentini, P. J. Klar, and W. Stolz, Phys. Rev. B **69**, 041201(R) (2004).
[7] G. Pettinari, F. Masia, A. Polimeni, M. Felici, A. Frova, M. Capizzi, A. Lindsay, E. P. O'Reilly, P. J. Klar, W. Stolz, G. Bais, M. Piccin, S. Rubini, F. Martelli, and A. Franciosi, Phys. Rev. B **74**, 245202 (2006).
[8] M. Henini, *Dilute Nitride Semiconductors* (Elsevier, Oxford, 2005).
[9] M. Felici, A. Polimeni, G. Salviati, L. Lazzarini, N. Armani, F. Masia, M. Capizzi, F. Martelli, M. Lazzarino, G. Bais, M. Piccin, S. Rubini, and A. Franciosi, Adv. Mater. (Weinheim, Ger.) **18**, 1993 (2006).
[10] R. Trotta, A. Polimeni, M. Capizzi, D. Giubertoni, M. Bersani, G. Bisognin, M. Berti, S. Rubini, F. Martelli, L. Mariucci, M. Francardi, and A. Gerardino, Appl. Phys. Lett. **92**, 221901 (2008).
[11] M. Geddo, T. Ciabattoni, G. Guizzetti, M. Galli, M. Patrini, A. Polimeni, R. Trotta, M. Capizzi, G. Bais, M. Piccin, S. Rubini, F. Martelli, and A. Franciosi, Appl. Phys. Lett. **90**, 091907 (2007).
[12] Y.-S. Kim and K. J. Chang, Phys. Rev. B **66**, 073313 (2002).
[13] A. Amore Bonapasta, F. Filippone, P. Giannozzi, M. Capizzi, and A. Polimeni, Phys. Rev. Lett. **89**, 216401 (2002).
[14] A. Janotti, S. B. Zhang, S.-H. Wei, and C. G. Van de Walle, Phys. Rev. Lett. **89**, 086403 (2002).
[15] F. Jiang, M. Stavola, M. Capizzi, A. Polimeni, A. Amore Bonapasta, and F. Filippone, Phys. Rev. B **69**, 041309(R) (2004).
[16] A. Amore Bonapasta, F. Filippone, and P. Giannozzi, Phys. Rev. B **68**, 115202 (2003).
[17] A. Amore Bonapasta, F. Filippone, and P. Giannozzi, Phys. Rev. B **69**, 115207 (2004).
[18] G. Ciatto, F. Boscherini, A. A. Bonapasta, F. Filippone, A. Polimeni, and M. Capizzi, Phys. Rev. B **71**, 201301(R) (2005).
[19] W. B. Fowler, K. R. Martin, K. Washer, and M. Stavola, Phys. Rev. B **72**, 035208 (2005).
[20] M.-H. Du, S. Limpijumnong, and S. B. Zhang, Phys. Rev. B **72**, 073202 (2005).
[21] G. Bisognin, D. De Salvador, A. V. Drigo, E. Napolitani, A. Sambo, M. Berti, A. Polimeni, M. Felici, M. Capizzi, M. Güngerich, P. J. Klar, G. Bais, F. Jabeen, M. Piccin, S. Rubini, F. Martelli, and A. Franciosi, Appl. Phys. Lett. **89**, 061904 (2006).
[22] A. Amore Bonapasta, F. Filippone, and G. Mattioli, Phys. Rev. Lett. **98**, 206403 (2007).
[23] M. Berti, G. Bisognin, D. De Salvador, E. Napolitani, S. Vangelista, A. Polimeni, M. Capizzi, F. Boscherini, G. Ciatto, S. Rubini, F. Martelli, and A. Franciosi, Phys. Rev. B **76**, 205323 (2007).
[24] S. Kleekajai, F. Jiang, K. Colon, M. Stavola, W. B. Fowler, K. R. Martin, A. Polimeni, M. Capizzi, Y. G. Hong, H. P. Xin, C. W. Tu, G. Bais, S. Rubini, and F. Martelli, Phys. Rev. B **77**, 085213 (2008).
[25] I. A. Buyanova, W. M. Chen, M. Izadifard, S. J. Pearton, C.

Bihler, M. S. Brandt, Y. G. Hong, and C. W. Tu, Appl. Phys. Lett. **90**, 021920 (2007).
[26] F. Boscherini, *Characterization of Semiconductor Heterostructures and Nanostructures* (Elsevier, New York, 2008).
[27] P. Fons, H. Tampo, A. V. Kolobov, M. Ohkubo, S. Niki, J. Tominaga, R. Carboni, F. Boscherini, and S. Friedrich, Phys. Rev. Lett. **96**, 045504 (2006).
[28] J. T.-Thienprasert, J. Nukeaw, A. Sungthong, S. Porntheeraphat, S. Singkarat, D. Onkaw, S. Rujirawat, and S. Limpijumnong, Appl. Phys. Lett. **93**, 051903 (2008).
[29] G. Bisognin, D. De Salvador, C. Mattevi, M. Berti, A. Drigo, G. Ciatto, L. Grenouillet, P. Duvaut, P. Gilet, and H. Mariette, J. Appl. Phys. **95**, 48 (2004).
[30] L. Grenouillet, C. Bru-Chevallier, G. Guillot, P. Gilet, P. Ballet, P. Duvaut, G. Rolland, and A. Million, J. Appl. Phys. **91**, 5902 (2002).
[31] G. Ciatto, F. Boscherini, F. D'Acapito, D. De Salvador, D. Batchelor, R. Carboni, L. Grenouillet, H. Mariette, and S. Mobilio, Phys. Scr. **T115**, 356 (2005).
[32] G. Bisognin, D. De Salvador, E. Napolitani, M. Berti, A. Polimeni, M. Capizzi, S. Rubini, F. Martelli, and A. Franciosi, J. Appl. Crystallogr. **41**, 366 (2008).
[33] L. Floreano, G. Naletto, D. Cvetko, R. Gotter, M. Malvezzi, L. Marassi, A. Morgante, A. Santaniello, A. Verdini, and F. Tommasini, Rev. Sci. Instrum. **70**, 3855 (1999).
[34] G. Ciatto, J.-C. Harmand, F. Glas, L. Largeau, M. Le Du, F. Boscherini, M. Malvestuto, L. Floreano, P. Glatzel, and R. A. Mori, Phys. Rev. B **75**, 245212 (2007).
[35] A. L. Ankudinov, B. Ravel, J. J. Rehr, and S. D. Conradson, Phys. Rev. B **58**, 7565 (1998).
[36] X. Gonze, R. Stumpf, and M. Scheffler, Phys. Rev. B **44**, 8503 (1991).
[37] D. Vanderbilt, Phys. Rev. B **41**, 7892 (1990).
[38] S. Baroni, A. D. Corso, S. de Gironcoli, P. Giannozzi, C. Cavazzoni, G. Ballabio, S. Scandolo, G. Chiarotti, P. Focher, A. Pasquarello, K. Laasonen, A. Trave, R. Car, N. Marzari, and A. Kokalj, http://www.pwscf.org/.
[39] F. Romanato, D. De Salvador, M. Berti, A. Drigo, M. Natali, M. Tormen, G. Rossetto, S. Pascarelli, F. Boscherini, C. Lamberti, and S. Mobilio, Phys. Rev. B **57**, 14619 (1998).
[40] R. Atanasov, F. Bassani, A. D'Andrea, and N. Tomassini, Phys. Rev. B **50**, 14381 (1994).
[41] X. Liu, A. Prasad, J. Nishio, E. R. Weber, Z. Liliental-Weber, and W. Walukiewicz, Appl. Phys. Lett. **67**, 279 (1995).
[42] X. Liu, A. Prasad, W. M. Chen, A. Kurpiewski, A. Stoschek, Z. Liliental-Weber, and E. R. Weber, Appl. Phys. Lett. **65**, 3002 (1994).
[43] R. M. Feenstra, J. M. Woodall, and G. D. Pettit, Phys. Rev. Lett. **71**, 1176 (1993).
[44] K. Kim and A. Zunger, Phys. Rev. Lett. **86**, 2609 (2001).
[45] V. Lordi, V. Gambin, S. Friedrich, T. Funk, T. Takizawa, K. Uno, and J. S. Harris, Phys. Rev. Lett. **90**, 145505 (2003).
[46] G. Ciatto, F. D'Acapito, L. Grenouillet, H. Mariette, D. De Salvador, G. Bisognin, R. Carboni, L. Floreano, R. Gotter, S. Mobilio, and F. Boscherini, Phys. Rev. B **68**, 161201(R) (2003).
[47] W. Ulrici and B. Clerjaud, Phys. Rev. B **72**, 045203 (2005).